Insect Biochemistry and Molecular Biology 39 (2009) 717–725

Contents lists available at ScienceDirect

Insect Biochemistry and Molecular Biology

journal homepage: www.elsevier.com/locate/ibmb

# Functions of ion transport peptide and ion transport peptide-like in the red flour beetle *Tribolium castaneum*

Khurshida Begum [a], Bin Li [a], Richard W. Beeman [b], Yoonseong Park [a,*]

[a] Department of Entomology, Kansas State University, 123 Waters Hall, Manhattan, KS 66506, USA
[b] USDA-ARS Grain Marketing and Production Research Center, 1515 College Avenue, Manhattan, KS 66502, USA

ARTICLE INFO

*Article history:*
Received 6 July 2009
Received in revised form
18 August 2009
Accepted 19 August 2009

*Keywords:*
Crustacean hyperglycemic hormone CHH
RNA interference
Reproduction
Neuropeptide
Beetle
Development

ABSTRACT

Ion transport peptide (ITP) and ITP-like (ITPL) are highly conserved neuropeptides in insects and crustaceans. We investigated the alternatively spliced variants of ITP/ITPL in *Tribolium castaneum* to understand their functions. We identified three alternatively spliced transcripts named *itp*, *itpl-1*, and *itpl-2*. Expression patterns of the splice variants investigated by exon-specific *in situ* hybridization were somewhat different from those previously reported in other insect species. Most importantly, we found for the first time that *itpl-1* transcripts are abundantly expressed in the midgut at the late larval stage, showing an expression pattern similar to that of the crustacean hyperglycemic hormone (CHH) in the crab *Carcinus maenas*. CHH was shown to function by increasing the body volume through fluid absorption, resulting in breakage of the outer shell at the time of molt. Exon-specific RNA interference (RNAi) was designed to distinguish between *itp* and *itpl-1*, but we were unable to design a dsRNA uniquely targeting or uniquely excluding *itpl-2*; therefore, RNAi targeting was limited to either *itp*/*itpl-2 or itpl-1*/*itpl-2*. For dsRNA injections in the larval stages, either RNAi led to gradually increasing mortality in the larval and pupal stages, with 100% cumulative mortality at the time of eclosion or shortly afterward. Developmental deficiencies in the adult tarsal segments were observed after RNAi suppressing either *itp*/*itpl-2* or *itpl-1*/*itpl-2*. After dsRNA injections at the pupal stage, the most striking observation was a significant reduction in egg numbers (8% of control) and reduced survival of the offspring (5%) in RNAi targeting *itpl-1*/*itpl-2*, while a milder degree of the same phenotype was observed in that targeting *itp*/*itpl-2*.

© 2009 Elsevier Ltd. All rights reserved.

## 1. Introduction

Neuropeptides and endocrine peptides are diffusible signaling molecules involved in many physiological, behavioral, and developmental events. Ion transport peptide (ITP) in locusts (*Schistocerca gregaria* and *Locusta migratoria*) was identified based on its antidiuretic activity in the ileum (Audsley et al., 1992, 2006). ITP, released from the endocrine organs known as the corpora cardiaca (CC), stimulates the ileum to transport $Cl^-$ ion from lumen to hemolymph, thus forming an electrochemical gradient driving water resorption. Cloning the gene encoding ITP identified an alternatively spliced exon encoding a homologous product distinguished by the lack of C-terminal amidation which occurs in ITP, and named ITP-like or ITPL (Phillips et al., 1998b).

ITP and ITPL in insects are homologous to a large family of endocrine peptides found in crustaceans (reviewed in Chen et al., 2005; Dircksen, 2009). These functionally diverse peptides are further grouped into crustacean hyperglycemic hormone (CHH), molt inhibiting hormone (MIH), vitellogenin-inhibiting hormone (VIH), and mandibular organ inhibition hormone (MOIH). All these peptides and ITP/ITPL are characterized by six strictly conserved cysteines, which have been shown to form three intramolecular disulfide bonds for the MIH of the kuruma prawn (Aguilar et al., 1996). In addition to the functions indicated by their names above, CHH is known to function at the time of crab molting, triggering fluid absorption which in turn enables the animal to break out of the old exoskeleton (Chung et al., 1999).

The genes encoding ITP and ITPL have been described in the lepidopteran and dipteran species *Bombyx mori*, *Manduca sexta*, *Aedes aegypti*, and *Drosophila melanogaster* (Dai et al., 2007; Dircksen et al., 2008; Drexler et al., 2007; Endo et al., 2000), in addition to earlier descriptions of cDNAs in Locust species (Meredith et al., 1996; Phillips et al., 1998b). While a clear functional description for locust ITP has been made using hindgut epithelial physiology to demonstrate the activation of $Cl^-$ absorption, other possible functions were suggested based on the expression patterns of ITP and ITPL in various cells of the central nervous system and the peripheral nervous system

* Corresponding author. Tel.: +1 785 532 5763.
*E-mail address:* ypark@ksu.edu (Y. Park).

0965-1748/$ – see front matter © 2009 Elsevier Ltd. All rights reserved.
doi:10.1016/j.ibmb.2009.08.005

(Dai et al., 2007; Dircksen et al., 2008; Drexler et al., 2007). A possible function for ITP/ITPL in molting has also been inferred in insects (Dai et al., 2007; Drexler et al., 2007).

We investigated a coleopteran insect, the red flour beetle (*Tribolium castaneum*), to examine the possibility of an essential role for ITP/ITPL. The whole genome sequence and a large expressed sequence tag database of this insect are publicly available (Park et al., 2008; Richards et al., 2008); ITP/ITPL were previously identified in an annotation of neuropeptides (Li et al., 2008). Systemic RNA interference (RNAi) has been highly successful in all stages of *T. castaneum* development including parental RNAi (Bucher et al., 2002; Tomoyasu and Denell, 2004; Tomoyasu et al., 2008). The RNAi technique has been successfully used for targeting neuropeptide signaling pathways in *T. castaneum*, examining their roles in diuresis and in ecdysis behavior (Aikins et al., 2008; Arakane et al., 2008). In this study, we investigated *itp*/*itpl* expression patterns and their functions in *T. castaneum* by using *in situ* hybridization and RNAi.

## 2. Materials and methods

### 2.1. Insect rearing and gene cloning

The Georgia-1 (GA-1) strain of *T. castaneum* was reared at 30 °C in 5% yeasted flour (Haliscak and Beeman, 1983). For reverse transcription-PCR (RT-PCR), specific primers designed based on our gene predictions were used (Table 1). The 5′ and 3′ ends of the cDNA were identified by nested PCR screening of a whole-body larval cDNA library (Park et al., 2008) using primers located in the vector sequence in conjunction with gene specific primers.

Total RNA was isolated from last-instar larvae using Trizol reagent (Invitrogen). First-strand cDNAs were synthesized by using the SuperScript III First-strand Synthesis kit (Invitrogen) with oligo $(dT)_{20}$ as primer. PCR products were cloned into the pGEM-T Easy Vector (Promega) and sequenced in the Core Instrument Facility at the University of California, Riverside. After we identified three alternatively spliced forms, we used exon-specific primers in subsequent studies. The exon-specificities were confirmed by using control clones encoding each isoform (data not shown). The sequences are available in GenBank with the following accession numbers: EF222298, EF222297, and EF222299 of *itp*, *itpl-1* and *itpl-2* respectively.

Phylogenetic analysis used MEGA4 (Tamura et al., 2007) for generation of a neighbor-joining tree to examine the evolutionary relationship between insect ITPs and its closely related CHH/MIH groups. The bootstrapping values were with 1000 samplings.

### 2.2. Quantitative real-time RT-PCR

Total RNA from a pool of 2 individuals was extracted from each of the following developmental stages: early embryo (EE, <24 h), late embryo (LE, >24 h), early larva (EL, <24 h post-hatching), late larva (LL, older than 5th instar including prepupae), early pupa (EP, <24 h post-pupation), late pupa (LP, >72 h post-pupation), early adult (Ead, <24 h post-eclosion), and late adult (Lad, one week old). To analyze tissue-specific expression, we collected total RNA from each of the following dissected tissues: CNS (central nervous system including brain and ganglia), gut (foregut, midgut, hindgut and Malpighian tubules), and carcass excluding the aforementioned tissues. A pool of five last-instar larvae was used for preparing each tissue. The splice variants *itpl-1* and *itpl-2* were distinguished by primers designed at the junctions of two specific exons, Exon 2 and 3a, or Exon 2 and 3b (Table 1). These primers were initially tested with clones for each splice variant to confirm their specificities. Real-time RT-PCR was performed by using the SYBR Green Kit (Takara). Data expressed here as relative mRNA levels were standardized to a control gene *ribosomal protein S3* (*rpS3*, GenBank accession numbers CB335975, using the ΔΔCT method (Livak and Schmittegen, 2001).

### 2.3. In situ hybridization

Three probes, *E2-common*, *E3a-itpl-1*, and *E3b-itp*, were designed for Exons 2, 3a, and 3b, respectively, by using the PCR DIG Probe Synthesis Kit (Roche). Single-stranded DNA was generated by using asymmetric PCR with the primers listed in Table 1. Sense (for negative control) and antisense probes were made by using forward and reverse primers, respectively.

Dissected central nervous system (CNS) or paraffin sections were used for *in situ* hybridization. Tissues were fixed in 4% paraformaldehyde at 4 °C, washed 3 × 15 min with PBST (PBS and 0.2% Triton-X-100), treated with 10 μg/mL proteinase K, re-fixed in 4% paraformaldehyde for 15 min, and hybridized at 48 °C for 20–30 h. After hybridization, tissues were washed with hybridization solution, blocked in 1% BSA (Bovine serum albumin), and incubated with anti-digoxigenin-alkaline phosphatase (Roche, 1:1000 dilution in 1% BSA) overnight at 4 °C. The tissues were then washed in alkaline phosphatase buffer

**Table 1**
List of primers used in this study.

| Name | Sequence (5′–3′) | Remarks |
|---|---|---|
| **RT-PCR and RACE** | | |
| TcITPL1-755F | ATGAATTACCGATCATCCAA | RT-PCR, RACE |
| TcITPL1-759R | CTAAATTAAGTTAGTGTGTTAG | RT-PCR, RACE, qRT-PCR |
| TcITP-754F | GTTGTTTTGTGGTAGTTTGC | RT-PCR |
| TcITP-760F | CGAGTGCTTCTCCACCAAAT | RACE |
| TcITP-761R | TTACTTCGATAAATATTCAATCA | RT-PCR, RACE |
| TcITPL1/2-973F | CCATAACTTATGCAGGAAAA | qRT-PCR |
| TcITP-974R | AGAAGCACTCGGACCTGCAT | qRT-PCR |
| TcITPL2R | TTACTTCGATAAATATTCAATCA | qRT-PCR |
| TcRPS3F | ACCGTCGTATTCGTGAATTGAC | qRT-PCR |
| TcRPS3R | ACCTCGATACACCATAGCAAGC | qRT-PCR |
| **dsRNA synthesis** | | |
| dsTcITP-E2F | TAATACGACTCACTATAGGGTTGTTTTGTGGTAGTTTGCA | |
| dsTcITP-E2R | TAATACGACTCACTATAGGGCATAAGTTATGGAGTTGTGG | |
| dsTcITPL1F | TAATACGACTCACTATAGGCGACAGATTACTTCAAAGGA | |
| dsTcITPL1R | TAATACGACTCACTATAGGCCAACTCAGCTCCACGTATT | |
| dsTcITPF | TAATACGACTCACTATAGGCGAGTGCTTCTCCACCAAAT | |
| dsTcITPR | TAATACGACTCACTATAGGTTACTTCGATAAATATTCAATCA | |

(100 mM NaCl, 50 mM $MgCl_2$, 100 mM Tris pH 9.5, 0.1% Tween 20) and the color was developed by adding the substrate nitroblue tetrazolium salt/5-bromo-4-chloro-3-indoyl phosphate (NBT/BCIP, Roche, 1:50 dilution in AP buffer). Color development was stopped by repeated washes with PBS, after which the tissues were mounted in 100% glycerol.

### 2.4. RNA interference

Double stranded RNAs (dsRNAs) were synthesized for the same three different target regions covered by the *in situ* probes, namely *E2-common* (Exon 2), *E3a-itpl-1* (Exon 3a), and *E3b-itp* (Exon 3b). Probe lengths were 293, 99, and 103 bp, respectively (Fig. 1). The sequences used for dsRNAs were unique according to searches of the Tribolium genome sequence, with maximum off-target matches of 16 consecutive bp. A total of 200 ng dsRNA in 200 nL was injected into the body cavity. DsRNA injections were made at three different developmental stages, namely ~4th instar larvae, penultimate-instar larvae, and 2-day-old pupae. Larval injections were followed by observations of noticeable morphological defects and mortality. Mortality occurring less than 5 days after injection was attributed to injection injury rather than target transcript knockdown. In general, mortality due to injection damage was <10%. Pupal injections, which did not cause any detectable defects in adult eclosion, were regarded as parental RNAi experiments (Bucher et al., 2002) and were followed by assessment of oviposition rates and progeny survival. Individuals in two replications of RNAi were utilized for single pair matings (five and seven pairs, respectively). Three-day ovipositions (13-day to 16-day-old females) were collected, counted and held for hatch-rate measurement and observation of development. Numbers of offspring were counted ~15 days after the eggs were collected. DsRNA-treated females were dissected 22 days after eclosion to assess ovarian development. Negative controls consisted of injections of either *vermilion* dsRNA or an equal volume of buffer only. Knockdown levels of target transcripts were examined in late pupae or young adults from total RNA obtained from pools of two individuals. Number of individuals/number of replications is indicated by "##/#" in Figs. 5 and 6.

## 3. Results

### 3.1. Alternatively spliced transcripts itp, itpl-1, and itpl-2

Homology-based searches and prediction of gene structure identified the *itp* open reading frame with homologous, alternatively

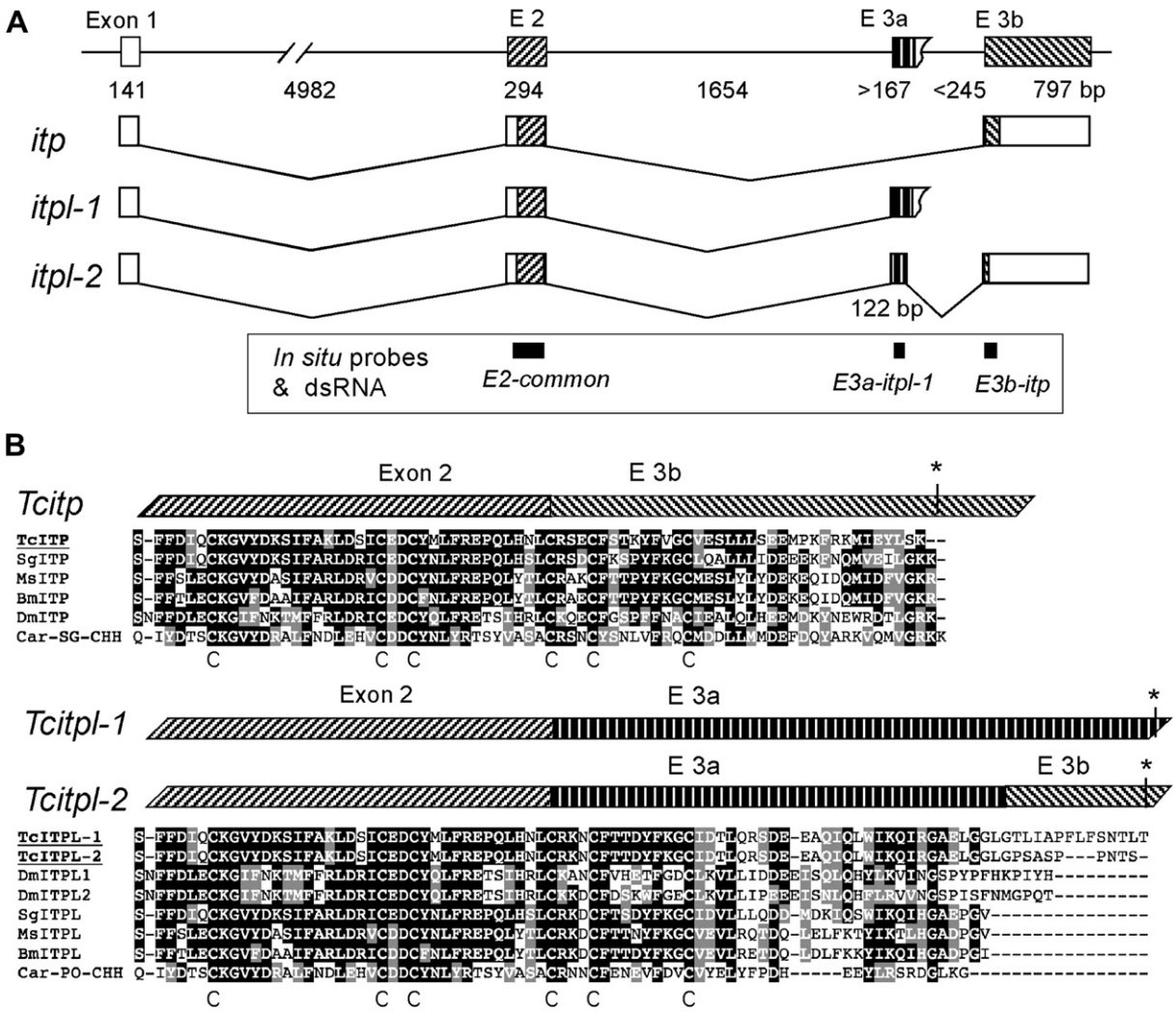


**Fig. 1.** Gene structure showing the alternatively spliced forms of *itp*, *itpl-1*, and *itpl-2* in *Tribolium castaneum* (A) and putative translations for mature peptide regions only, aligned with other homologous ITP/ITPL and CHH sequences (B). Alternative exons are marked with differently hatched lines. Box shade uses 50% the majority rule for identical (inverted in black box) and similar (inverted in gray box) amino acids in the multiple alignment.

spliced Exons 3a and 3b (Fig. 1A). The prediction was followed by 3′ and 5′ RACE. In RT-PCR with a primer located in Exon 3b, we identified an additional band. Sequence analysis of this band revealed an alternatively spliced form using both Exon 3a and 3b, which we named *itpl-2* (Fig. 1A and B). *Itpl-2* uses Exon 3a but jumps to Exon 3b before the reading frame reaches the stop codon in Exon 3a. This splicing results in a frameshift in Exon 3b and leads to a stop codon after 9 amino acid residues. Therefore, the translation of *itpl-2* differs from that of *itpl-1* by 13 amino acids at the C-terminus. A mild degree of similarity was found between 23 amino acid residues encoded by Exon 3b (ITP) and 43 amino acid residues encoded by Exon 3a (ITPL1 or 2, Fig. 1B). The cDNA ends of each transcript were identified by respective independent 3′ rapid amplification of cDNA ends (RACE), except for the 3′ end of *itpl-1*, which multiple approaches failed to identify. For the *itpl-1* transcript, a primer spanning the putative stop codon was used to confirm the annotation. All three splice variants share a 5′ transcription initiation site. *Itp* and *itpl-1* use Exon 3b and 3a, respectively, with stop codons occurring in each exon. All exon–intron junctions utilize GT and (C/T)AG consensus sequences for intron donor and acceptor, respectively.

Sequence alignment of putative ITP, ITPL1, and ITPL2 with ITP/ITPL of other insects and CHH revealed highly conserved sequences with clear cladistic distinction between ITP and ITPL in the alternatively spliced exon (Fig. 2). Other examples of exon duplications of ITPL into ITPL1 and ITPL2 have been found only in *Drosophila* species (Fig. 2) (Dircksen et al., 2008). The prohormone sequences contain N-terminal dibasic cleavage sites. Six cysteines in the putative mature peptides are strictly conserved. The C-terminal canonical amidation and dibasic cleavage signals (-GKK, -GKR, and -GRK) are also strictly conserved in previously published *itp* translations. Only *Tribolium* ITP lacks these motifs, ending instead with – YLSK, immediately followed by the stop codon. This sequence lacking the canonical amidation signal in *T. castaneum itp* has been confirmed in the genome sequence and multiple cDNA clones that we amplified in independent RT-PCR and in a cDNA library; thus, the lack of an amidation signal in *T. castaneum itp* does not appear to involve sequencing errors.

### 3.2. Expression patterns of itp variants

Quantitative real-time RT-PCR (qRT-PCR) provided general patterns of expression for each splice variant of *itp*. Primers located in the junctions between exons were used to amplify differently spliced forms by qRT-PCR (Fig. 3A). All three variants reached peak expression in the early pupal stages, while their embryonic expression levels were very low (Fig. 3B). Expression levels were generally reduced in the pupal and adult stages. Tissue-specific expression analysis in the last larval instar revealed high expression of *itp* in the CNS, while *itpl-1* and *-2* were expressed equally in CNS, gut and carcass (Fig. 3B). Since the mRNA levels shown in Fig. 3B are relative to levels in the early larval stages (for life-stage comparisons) or in carcass (for tissue comparisons), it is important to emphasize that quantitative comparisons among different isoforms are not justifiable using these data because amplification efficiencies during RT-PCR for each isoform may vary. However, with the above caution, it is noteworthy to mention that we consistently had relatively low levels of amplification of *itpl-2*, implying that *itpl-2* may have low levels of expression. After RT-PCR using primers located in E3a (forward) and E3b (reverse), we identified the band only for the *itpl-2* transcript, but not for *itpl-1*, indicating that the 3′ end of *itpl-1* does not extend to E3b (Figs. 1 and 3).

*In situ* hybridization provided further insights into tissue- and cell-specific expression patterns. The probe from Exon 2 (*E2-common*, Fig. 1) should hybridize to all three variants, while probes from Exon 3a (*E3a-itpl-1*) and 3b (*E3b-itp*) should hybridize specifically to *itpl-1* or *itp*, respectively. The *itpl-2* transcript utilizes both Exon 3a and 3b, thus should hybridize to all three probes.

We found strong hybridization signal in 5 pairs of brain cells on the dorsal side of the protocerebral hemispheres and in a pair of

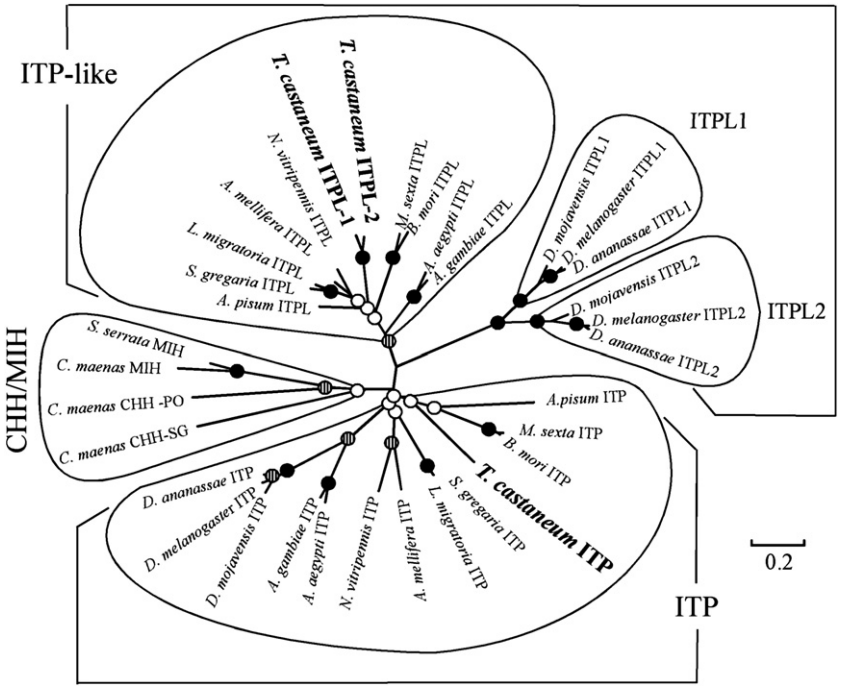


**Fig. 2.** Neighbor-joining tree showing the evolutionary relationship of CHH/ITP/ITPL. Circles at nodes are bootstrapping supports for higher than 90% (filled), between 90% and 50% (hatched), and lower than 50% (empty). Note that the alternative exons specifying ITPL1 or ITPL2 occur only in *Drosophila* species, while *T. castaneum* ITPL1 and ITPL2 are isoforms generated by overlapping exons.

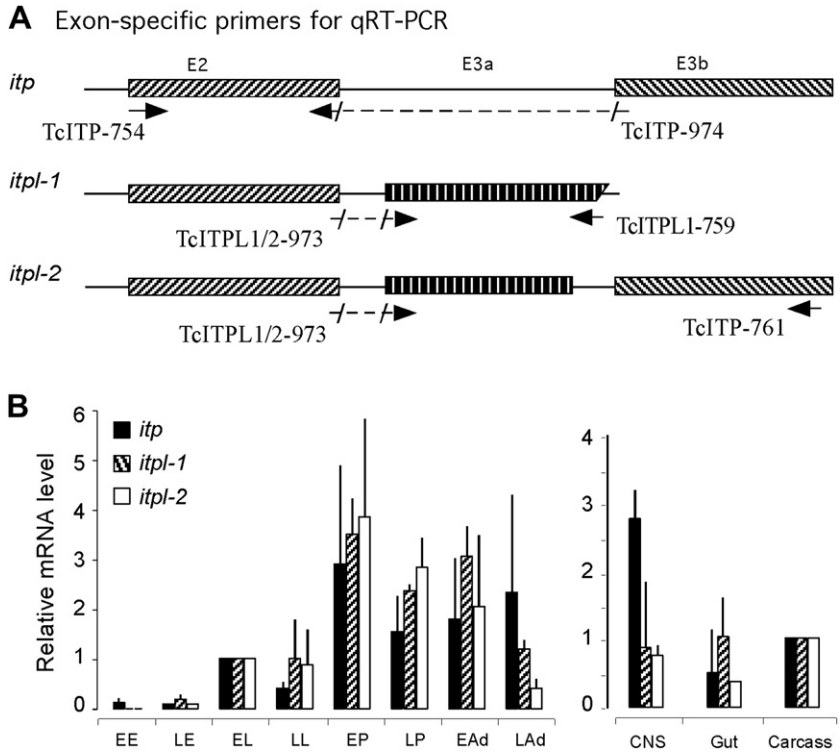


**Fig. 3.** Exon-specific primers designed for discriminating alternatively spliced forms *itp*, *itpl-1*, and *itpl-2* in *Tribolium castaneum* (A) and quantitative RT-PCR shown as relative expression levels normalized by rpS3 (B). The specific primers were designed in the junctions of alternatively spliced exons (connected by dotted lines). The qRT-PCR results are shown as levels relative to those of the early larval stage (EL) for the temporal expression levels and to those of carcass for the tissue-specific expression levels. Standard error bars represent three replicates.

cells in the terminal abdominal ganglion with probes *E2-common* and *E3b-itp*, but not with *E3a-itpl-1* (Fig. 4A–F). Identical patterns of staining were found in larval, pupal, and adult brains. *E3a-itpl-1* hybridization was found in midgut cells and in unidentified paired segmental cells in a peripheral tissue presumed to be peripheral nervous system (PNS) (Fig. 4G–I). Specifically, these cells were negative for *E3b-itp* staining, implying that only *itpl-1* is expressed. The *E3a-itpl-1* positive gut cells were found only in the prepupal stage in 4 out of 9 samples (3 replications for 3 guts for each), while no insects from the earlier stage (last larval instar) showed any positive signal ($n = 14$ in 3 replications). There was no staining pattern indicating hybridization of the same cells to both probes *E3b-itp* and *E3a-itpl-1*, which would be expected of *itpl-2* transcripts. All the cells described above were hybridized by *E2-common*. We therefore conclude that there were no *itpl-2* transcripts detectable by *in situ* hybridization.

### 3.3. RNAi phenotype

Knock down levels of target transcripts were examined by RT-PCR using a pool of two individuals for each treatment 5 days after dsRNA injections into late-instar larvae (Fig. 5B). Injection of *E2-common* suppressed all three isoforms, while exon-specific RNAi knocked down *itpl-1* or *itp* after injection of dsRNA *E3a-itpl-1* or *E3b-itp*, respectively. *Itpl-2* utilizing both Exons 3a and 3b was suppressed by either exon-specific dsRNA. Consistent results were obtained during RT-PCR confirmations in three replications of RNAi by two different researchers.

Injection of dsRNAs into penultimate-instar larvae caused steadily increasing mortality, reaching nearly 100% by the time of adult eclosion. Approximately 20% of insects died before pupation in both *ds-itpl-1* and *ds-itp* treatments. A large portion (~15–30%) of dsRNA-treated insects died during the pupal stage. Most treated insects died at the time of adult eclosion with incomplete shedding of the pupal cuticle (Fig. 5A and C). Rarely, successful eclosion occurred, but death usually ensued within 2 days (Fig. 5C).

We also found a developmental defect in the beetles surviving until the pharate adult stage in the injections of either *ds-E3a-itpl-1* or *ds-E3b-itp*. Such insects failed to form normal terminal tarsal segments of adult legs (Fig. 5D). The deficiencies in the formation and tanning of the tarsal segments were observed in all six legs with slightly varying degrees of severity.

In order to examine later stages for RNAi phenotypes, we injected two-day-old pupae and assessed survivorship, oviposition rate and the survivorship of offspring. All insects treated as pupae with either *ds-E3a-itpl-1* or *ds-E3b-itp* eclosed normally. In both cases, mortality increased gradually during adult life compared to the control, resulting in less than 35% survivorship 26-day after eclosion (Fig. 6).

RNAi of *E3a-itpl-1* or *E3b-itp* in the pupal stage caused a significant reduction in egg production and progeny survival, with the former causing a more severe phenotype (Fig. 7A and B). The oviposition rates following dsRNA targeting ITPL and ITP were reduced to 8% and 27% of the control rate of ~8 eggs/day/female. We found that the RNAi resulted in defects in development of the ovary (Fig. 7C, representative picture of $n = 4$–6 for each treatment). Reduction in the number of eggs was more pronounced after injection of *ds-E3a-itpl-1* than of *ds-E3b-itp*, consistent with our observation of more severe developmental defects of ovary associated with *ds-E3a-itpl-1*. In dissections of treated females, we found that the individuals subjected to *itpl-1*/*itpl-2* RNAi have reduced ovaries that lack mature ovarioles (Fig. 7C). Individuals subjected to *itp*/*itpl-2* RNAi had fully developed ovaries, whereas reduced oviposition rates and offspring survival were observed

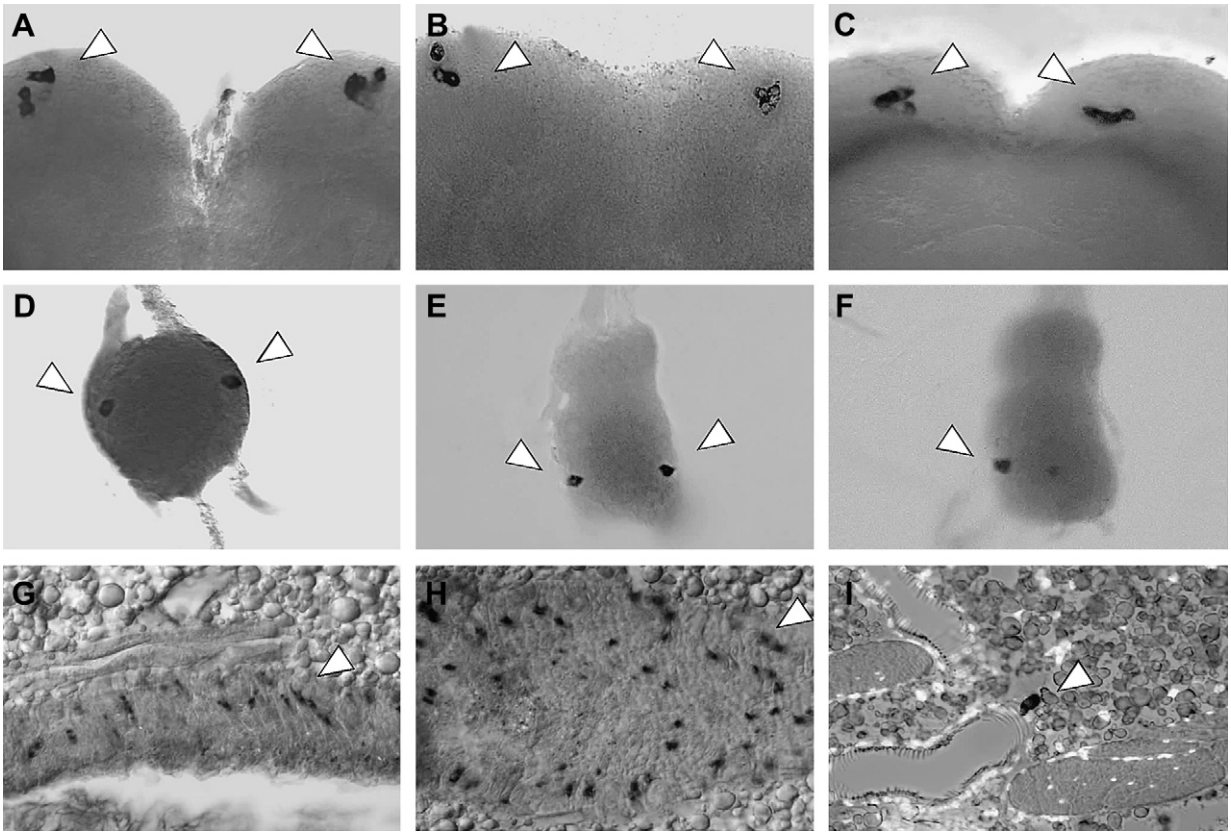


**Fig. 4.** *In situ* hybridization showing positive cells for the probes *E3b-itp* in the larval (A, D), pupal (B, E), and adult (C, F) stages in the brain (A, B, C) and in the terminal abdominal ganglion (D, E, F). Positive cells for the *E3a-itpl-1* probe in the midgut layer (G, H), and a peripheral cell that is thought to be a peripheral neuronal cell (I) are indicated by arrowheads. Top corresponds to anterior for A to F. G shows a longitudinal section of the midgut epithelial layer oriented with the lumen side down. H is a part of a longitudinal section of the midgut. Note that the cells in peripheral tissue (i.e., I) were observed in a segmentally repeated manner in the reconstruction of multiple layers of successive microtome sections. The regions for exon-specific probes are shown in Fig. 1.

(Fig. 7C). We found fully developed eggs stuck in the lateral oviducts (3 out of 4 dissected individuals), while eggs in the lateral oviduct were never observed in dissections of wild-type or control beetles. Significant reductions in hatching/survivorship were observed after injections of *E3a-itpl-1* and *E3b-itp* (5% and 63% survivorship, respectively).

## 4. Discussion

ITP was originally isolated based on its activity promoting $Cl^-$ absorption in *Locust ileum*. Subsequently, a splice variant ITP-like (ITPL) was identified during gene cloning (Audsley et al., 1992; Phillips et al., 1998a,b). Genome sequences of a number of insect species revealed that ITP and ITPL are highly conserved peptides (Dircksen, 2009). Recent studies of ITP and ITPL in moths (Dai et al., 2007; Drexler et al., 2007; Endo et al., 2000) and fruitfly (Dircksen et al., 2008) have focused on expression patterns using immunohistochemistry and *in situ* hybridization. Our study of ITP/ITPL in *T. castaneum* provides a unique opportunity to examine the hypo- or amorphic phenotypes of these neuropeptides by using the RNAi technique, adding to our understanding of their functions.

### *4.1. Tissue-specific expression patterns in T. castaneum compared to those in other insect species*

The patterns of staining after exon-specific *in situ* hybridization in this study could be interpreted in terms of expression patterns of three alternatively spliced forms. As previously mentioned, the *itp* transcript should hybridize to both probes *E2-common* and *E3b-itp*, while the *itpl-1* transcript should hybridize to the probes *E2-common* and *E3a-iptl-1*. The *itpl-2* transcript could hybridize to all three probes *E2-common*, *E3a-itpl-1*, and *E3b-itp*, but such a pattern of hybridization was not detected in this study. We found that *itp* was expressed exclusively in 5 pairs of protocerebral cells and a pair of abdominal terminal ganglion cells (Fig. 4A–F). *Itpl-1* was expressed in the peripheral nervous system (Fig. 4I), and also in midgut endocrine cells, only at the late larval stage (Fig. 4G and H).

In general, expression patterns of *itp* and *itpl* were similar to those described in *B. mori*, *M. sexta* and *D. melanogaster* (reviewed in Dircksen, 2009). *Itp* expression in the 5 pairs of protocerebral cells was commonly observed in other species (4 pairs in *D. melanogaster*, Dircksen et al., 2008). A pair of cells expressing *itp* in the terminal abdominal ganglion of *T. castaneum* may be homologous to the ITP-expressing segmental cells in the terminal abdominal region in *D. melanogaster* (Dircksen et al., 2008), while moths (*M. sexta* and *B. mori*) have segmental nervous cells for ITPL, but not for ITP (Dai et al., 2007; Drexler et al., 2007). Cells in the peripheral nervous system, which were positive for ITPL in moths and fruitflies, were also stained in *T. castaneum*. A strong *itpl-1* positive signal was found in the bilaterally symmetric segmental cells in microtome sections of larval stages (Fig. 4I). Since we have not been able to obtain reliable results from immunohistochemisty in this species using a Mas-ITP antibody (Dai et al., 2007), we were unable to describe the projection patterns of the neural cells. Based on previous immunohistochemical studies in other insects, the protocerebral cells may have projections to the corpora cardiaca and

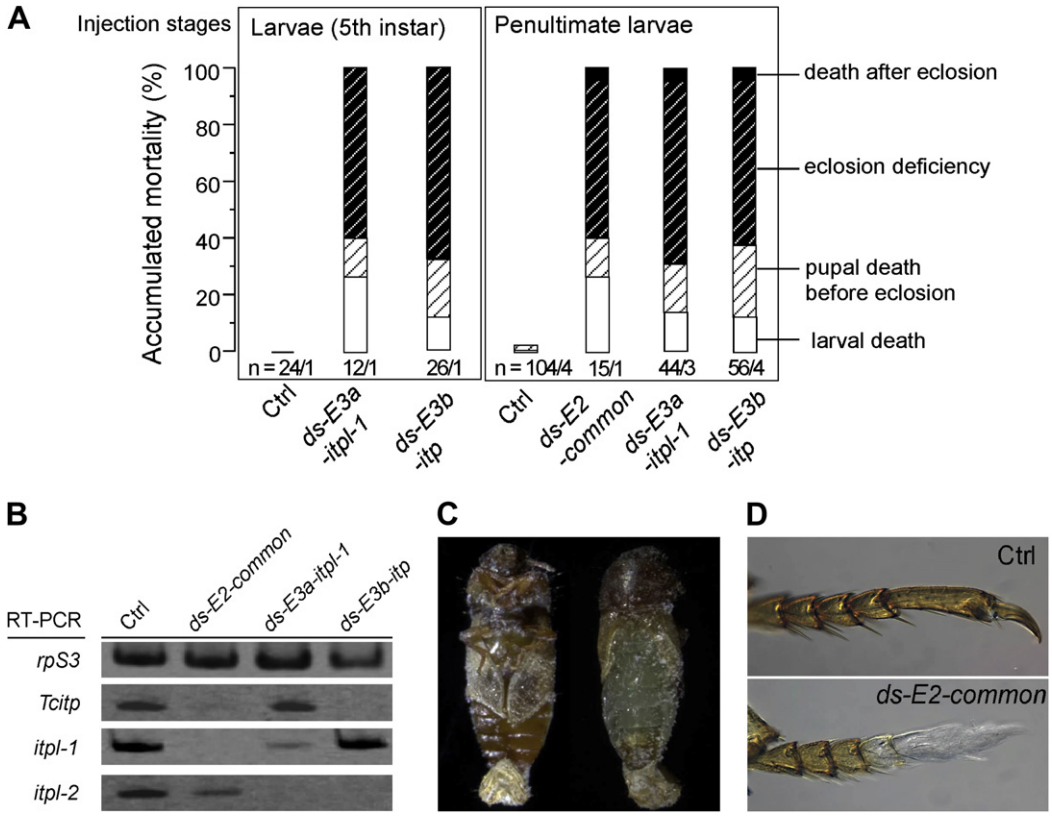


**Fig. 5.** RNA interference resulting in progressively increasing mortalities in three different RNAi tests at two different injection-stages (A). RNAi results of suppression of the respective mRNA shown by semi-quantitative RT-PCR (B). Representative lethal phenotypes (C). The defect in the tarsal development in RNAi (D). (B) shows typical results from 3 replications. The $n$ = "##/#" indicates the number of individuals/number of replications.

corpora allata, and the cells in abdominal terminal ganglion probably have projections to the hindgut (Dircksen et al., 2008) and possibly to reproductive organs based on our RNAi phenotype in this study.

A striking contrast between results of this study and those from previous studies in *B. mori*, *M. sexta*, and *D. melanogaster* is expression of *itpl-1* in numerous cells in the *Tribolium* midgut just prior to pupation. The midgut expression of *itpl-1* is particularly interesting because it may be homologous to the CHH expression system in the gut of the crab *Carcinus maenas*, which functions in ion and water uptake, causing body swelling during molting (Chung et al., 1999). Previous studies in *M. sexta* specifically examined the gut expression of CHH-like or ITP/ITPL, but did not detect any immunoreactivity in this tissue (Dai et al., 2007; Drexler et al., 2007). This difference could reflect differences in the developmental stages chosen for immunohistochemical analysis, in addition to possible species-specific differences.

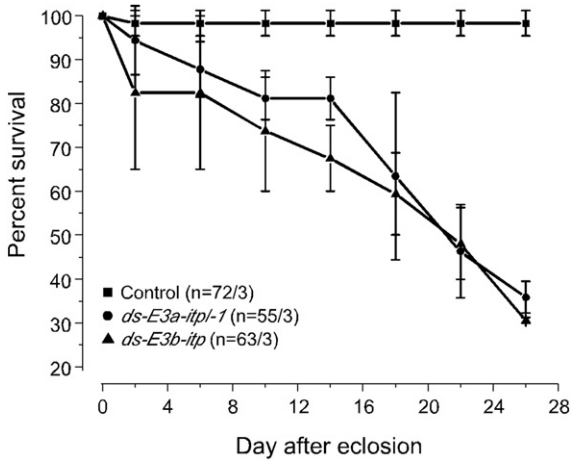


**Fig. 6.** Cumulative adult mortality after injection of respective dsRNAs in two-day-old pupae. "##/#" indicates the number of individuals/number of replications. The error bars are for standard deviations of three replicates.

### 4.2. Functions of differently spliced exons

A number of studies have attempted to detect a function of ITP/ITPL in insect molting based on the earlier finding of CHH activation of water absorption, increasing the body volume in order to split the old cuticle in a crab (Chung et al., 1999). The function of ITP in locust for $Cl^-$ ion mediated water resorption in the ileum has been clearly documented (Audsley et al., 1992), although it is unknown whether ITP in locust is involved in molting. Insect molting coincides with a rapid absorption of molting fluid from the space between the old and new cuticle layers. Withdrawal of molting fluid is likely equivalent to the tracheal airfill in larval molting of *D. melanogaster*, the white head stage during adult eclosion of *D. melanogaster*, and the air-filled head capsule during larval molting of *M. sexta*, and occurs shortly before the sequence of pre-ecdysis and ecdysis behaviors (Park et al., 1999, 2002; Zitnan et al., 1999). A previous study in *M. sexta* described an increase in CHH-immunoreactivity in the hemolymph coinciding with decreased CHH-immunoreactivity of perivisceral organs during the molt from the 4th to 5th instar larva (Drexler et al., 2007). Although immunohistochemical quantification may suffer from low accuracy, these results suggest the release of ITPL from thoracic cells into the hemolymph at the time of molting.

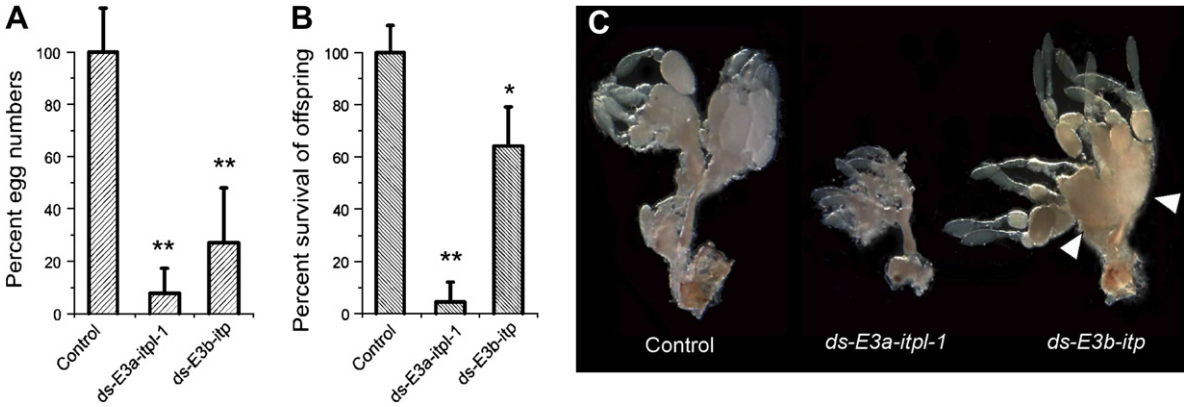


**Fig. 7.** Reduced egg laying (A) and survivorship in the offspring (B) associated with developmental defects of the ovary (C) after RNAi. Confidence intervals calculated using Student-*t* test for 12 single pair mating and show standard deviations and significant differences compared to the control using ** for $p < 0.01$ and * for $p < 0.05$. Arrowheads in C indicate the lateral oviducts clogged by mature eggs.

We find that ITP/ITPL in *T. castaneum* have an important function in adult eclosion, whereas they are less important for larval–larval or larval–pupal molting. RNAi for either *itp*/*itpl-2* or *itpl-1*/*itpl-2* resulted in an identical major defect in adult eclosion with less than 40% lethality in earlier stages. One possible explanation for the eclosion deficiency could be defects in shedding the old tracheae, although this possibility needs to be critically examined.

Malformation of adult tarsal segments was observed after dsRNA treatments. Interestingly, a defect in development of tibia and tarsal segments was induced by ablation of periodic abdominal pumping in the pupal stage in a larger tenebrionid beetle *Zoophoba atratus* (Ichikawa, 2008). Denervation of the ventral nerve cord caused this phenotype, while this defect was rescued by artificial rhythmic abdominal bending. Based on these observations, ITP/ITPL may be involved in activation of the periodic abdominal movements associated with pre-ecdysis.

Larval RNAi resulted in about 30% mortality prior to adult eclosion. These deaths were not associated with larval or pupal molting, implying that ITP/ITPL is not essential for larval–larval, or larval–pupal molting in *T. castaneum*. Pupal RNAi led to an accumulated 60% mortality by 26 days post-eclosion, but we were unable to determine the cause of these deaths. We conclude that ITP/ITPL is probably required throughout all life stages, although it may not be critical for immediate life-or-death, except for an essential role at the time of eclosion.

In our RNAi studies, associating specific splicing variants with deficiencies and mortality was not possible because *itpl-2* is targeted by all three exon-specific dsRNA regions, and no dsRNA uniquely targets or uniquely excludes *itpl-2*. However, we speculate that an important role for *itpl-2* is unlikely because the spliced form of *itpl-2* has not been found in other species, implying that it is probably not under constraining selection. The expression levels of *itpl-2* were lower than those of other splice variants by qRT-PCR, and tissue- or cell-specific expression for *itpl-2* was not detected.

Two different RNAi tests showed striking differences in reproductive effects. Dramatic decreases in egg numbers and in survival of the eggs was found after RNAi for *itpl-1*/*itpl-2*, while lower but significant reductions in these parameters were observed after RNAi for *itp*/*itpl-2*. The individuals subjected to *itpl-1*/*itpl-2* RNAi have reduced ovaries that lack mature ovarioles (Fig. 7C). This developmental defect may be caused by a hormonal imbalance for ovarian development. Alternatively, it could be indirectly caused by deficiencies in mating, preventing exposure to male ejaculatory products essential for completion of ovarian development. Individuals subjected to *itp*/*itpl-2* RNAi had fully developed ovaries, but showed reduced oviposition rates and offspring survival (Fig. 7C). Some fully developed eggs remained stuck in the lateral oviducts, while such eggs in the lateral oviduct were never observed in dissections of wild-type or control beetles. These observations, together with the presence of a pair of *itp* cells in the abdominal terminal ganglion, indicate that ITP may be involved in oviposition, possibly in activation of the oviduct for egg laying.

In summary, we have identified a novel splice variant of *itp*/*itpl* in addition to the variants described in other insect species. Another significant observation is expression of *itpl-1* in the midgut just before pupation, which has not been described in other insect species. RNAi indicates that ITP/ITPL are required throughout all life stages and are essential for adult eclosion. They are also involved in reproduction and offspring survival, and appear to function as peptide signals for multiple purposes in multiple life stages in *T. castaneum*.

## Acknowledgements

We thank Dr. Kun Yan Zhu and anonymous reviewers for their constructive criticisms of an earlier version of this paper. This work was supported by USDA-NRI-CSREES 2007-35604-17759. This article is contribution no. 09-351-J from the Kansas Agricultural Experiment Station. All programs and services of the US Department of Agriculture are offered on a nondiscriminatory basis, without regard to race, color, national origin, religion, sex, age, marital status or handicap. Mention of trade names or commercial products in this publication is solely for the purpose of providing specific information and does not imply recommendation or endorsement by the US Department of Agriculture.

## References

Aguilar, M.B., Falchetto, R., Shabanowitz, J., Hunt, D.F., Huberman, A., 1996. Complete primary structure of the molt-inhibiting hormone (MIH) of the Mexican crayfish *Procambarus bouvieri* (Ortmann). Peptides 17 (3), 367–374.

Aikins, M.J., Schooley, D.A., Begum, K., Detheux, M., Beeman, R.W., Park, Y., 2008. Vasopressin-like peptide and its receptor function in an indirect diuretic signaling pathway in the red flour beetle. Insect Biochemistry and Molecular Biology 38 (7), 740–748.

Arakane, Y., Li, B., Muthukrishnan, S., Beeman, R.W., Kramer, K.J., Park, Y., 2008. Functional analysis of four neuropeptides, EH, ETH, CCAP and bursicon, and their receptors in adult ecdysis behavior of the red flour beetle, *Tribolium castaneum*. Mechanisms of Development 125 (11–12), 984–995.

Audsley, N., McIntosh, C., Phillips, J.E., 1992. Actions of ion-transport peptide from locust corpus cardiacum on several hindgut transport processes. Journal of Experimental Biology 173, 275–288.

Audsley, N., Meredith, J., Phillips, J.E., 2006. Haemolymph levels of *Schistocerca gregaria* ion transport peptide and ion transport-like peptide. Physiological Entomology 31 (2), 154–163.

Bucher, G., Scholten, J., Klingler, M., 2002. Parental RNAi in Tribolium (Coleoptera). Current Biology 12 (3), R85–R86.

Chen, S.H., Lin, C.Y., Kuo, C.M., 2005. In silico analysis of crustacean hyperglycemic hormone family. Marine Biotechnology (New York) 7 (3), 193–206.

Chung, J.S., Dircksen, H., Webster, S.G., 1999. A remarkable, precisely timed release of hyperglycemic hormone from endocrine cells in the gut is associated with ecdysis in the crab *Carcinus maenas*. Proceedings of the National Academy of Sciences of the United States of America 96 (23), 13103–13107.

Dai, L., Zitnan, D., Adams, M.E., 2007. Strategic expression of ion transport peptide gene products in central and peripheral neurons of insects. Journal of Comparative Neurology 500 (2), 353–367.

Dircksen, H., 2009. Insect ion transport peptides are derived from alternatively spliced genes and differentially expressed in the central and peripheral nervous system. Journal of Experimental Biology 212 (3), 401–412.

Dircksen, H., Tesfai, L.K., Albus, C., Naessel, D.R., 2008. Ion transport peptide splice forms in central and peripheral neurons throughout postembryogenesis of *Drosophila melanogaster*. Journal of Comparative Neurology 509 (1), 23–41.

Drexler, A.L., Harris, C.C., dela Pena, M.G., Asuncion-Uchi, M., Chung, S., Webster, S., Fuse, M., 2007. Molecular characterization and cell-specific expression of an ion transport peptide in the tobacco hornworm, *Manduca sexta*. Cell & Tissue Research 329 (2), 391–408.

Endo, H., Nagasawa, H., Watanabe, T., 2000. Isolation of a cDNA encoding a CHH-family peptide from the silkworm *Bombyx mori*. Insect Biochemistry and Molecular Biology 30 (5), 355–361.

Haliscak, J.P., Beeman, R.W., 1983. Status of malathion resistance in 5 genera of beetles infesting farm-stored corn, wheat, and oats in the United-States. Journal of Economic Entomology 76 (4), 717–722.

Ichikawa, T., 2008. Periodic abdominal pumping supports leg development during metamorphosis in tenebrionid beetle *Zophobas atratus*. Comparative Biochemistry and Physiology A, Molecular & Integrative Physiology 150 (1), 8–13.

Li, B., Predel, R., Neupert, S., Hauser, F., Tanaka, Y., Cazzamali, G., Williamson, M., Arakane, Y., Verleyen, P., Schoofs, L., Schachtner, J., Grimmelikhuijzen, C.J.P., Park, Y., 2008. Genomics, transcriptomics, and peptidomics of neuropeptides and protein hormones in the red flour beetle *Tribolium castaneum*. Genome Research 18 (1), 113–122.

Livak, K.J., Schmittegen, T.D., 2001. Analysis of relative gene expression data using real-time quantitative PCR and the $2^{-\Delta\Delta Ct}$ method. Methods 25, 402–408.

Meredith, J., Ring, M., Macins, A., Marschall, J., Cheng, N.N., Theilmann, D., Brock, H.W., Phillips, J.E., 1996. Locust ion transport peptide (ITP): primary structure, cDNA and expression in a baculovirus system. Journal of Experimental Biology 199 (5), 1053–1061.

Park, Y., Aikins, J., Wang, L.J., Beeman, R.W., Oppert, B., Lord, J.C., Brown, S.J., Lorenzen, M.D., Richards, S., Weinstock, G.M., Gibbs, R.A., 2008. Analysis of transcriptome data in the red flour beetle, *Tribolium castaneum*. Insect Biochemistry and Molecular Biology 38 (4), 380–386.

Park, Y., Filippov, V., Gill, S.S., Adams, M.E., 2002. Deletion of the ecdysis-triggering hormone gene leads to lethal ecdysis deficiency. Development 129 (2), 493–503.

Park, Y., Zitnan, D., Gill, S.J., Adams, M.E., 1999. Molecular cloning and biological activity of ecdysis-triggering hormones in *Drosophila melanogaster*. FEBS Letters 463 (1–2), 133–138.

Phillips, J.E., Meredith, J., Audsley, N., Richardson, N., Macins, A., Ring, M., 1998a. Locust ion transport peptide (ITP): a putative hormone controlling water and ionic balance in terrestrial insects. American Zoologist 38 (3), 461–470.

Phillips, J.E., Meredith, J., Audsley, N., Ring, M., Macins, A., Brock, H., Theilmann, D., Littleford, D., 1998b. Locust ion transport peptide (ITP): function, structure, cDNA and expression. Recent Advances in Arthropod Endocrinology, 210–226.

Richards, S., Gibbs, R.A., Weinstock, G.M., Brown, S.J., Denell, R., Beeman, R.W., Bucher, G., Friedrich, M., Grimmelikhuijzen, C.J.P., Klingler, M., Lorenzen, M., Roth, S., Schroder, R., Tautz, D., Zdobnov, E.M., Consortium, T.G.S., 2008. The genome of the model beetle and pest *Tribolium castaneum*. Nature 452 (7190), 949–955.

Tamura, K., Dudley, J., Nei, M., Kumar, S., 2007. MEGA4: molecular evolutionary genetics analysis (MEGA) software version 4.0. Molecular Biology and Evolution 24 (8), 1596–1599.

Tomoyasu, Y., Denell, R.E., 2004. Larval RNAi in Tribolium (Coleoptera) for analyzing adult development. Development Genes and Evolution 214 (11), 575–578.

Tomoyasu, Y., Miller, S.C., Tomita, S., Schoppmeier, M., Grossmann, D., Bucher, G., 2008. Exploring systemic RNA interference in insects: a genome-wide survey for RNAi genes in Tribolium. Genome Biology 9 (1).

Zitnan, D., Ross, L.S., Zitnanova, I., Hermesman, J.L., Gill, S.S., Adams, M.E., 1999. Steroid induction of a peptide hormone gene leads to orchestration of a defined behavioral sequence. Neuron 23 (3), 523–535.